ARTICLE

$[Gd@C_{82}(OH)_{22}]_n$ Nanoparticles Induce Dendritic Cell Maturation and Activate Th1 Immune Responses

De Yang,[†,‡] Yuliang Zhao,[§] Hua Guo,[†] Yana Li,[‡] Poonam Tewary,[‡] Gengmei Xing,[§,*] Wei Hou,[†] Joost J. Oppenheim,[‡] and Ning Zhang[†,*]

[†]Tianjin Medical University, Research Center of Basic Medic Sciences, Cancer Institute and Hospital, Key Laboratory of Breast Cancer Research (Ministry of Education), Tianjin 300060, China, [‡]Basic Research Program, SAIC-Frederick, Inc., Laboratory of Molecular Immunoregulation, Cancer and Inflammation Program, Center for Cancer Research, National Cancer Institute at Frederick, Frederick, Maryland 21702, and [§]Key Laboratory for Biomedical Effects of Nanomaterials and Nanosafety, Institute of High Energy Physics, Chinese Academy of Sciences, Beijing 100049, China, and National Center for Nanoscience and Technology of China

ABSTRACT Dendritic cells play a pivotal role in host immune defense, such as elimination of foreign pathogen and inhibition of tumorigenesis. In this paper, we report that $[Gd@C_{82}(OH)_{22}]_n$ could induce phenotypic maturation of dendritic cells by stimulating DC production of cytokines including IL-12p70, upregulating DC co-stimulatory (CD80, CD83, and CD86) and MHC (HLA-A,B,C and HLA-DR) molecules, and switching DCs from a CCL5-responsive to a CCL19-responsive phenotype. We found that $[Gd@C_{82}(OH)_{22}]_n$ can induce dendritic cells to become functionally mature as illustrated by their capacity to activate allogeneic T cells. Mice immunized with ovalbumin in the presence of $[Gd@C_{82}(OH)_{22}]_n$ exhibit enhanced ovalbumin-specific Th1-polarized immune response as evidenced by the predominantly increased production of IFNγ, IL-1β, and IL-2. The $[Gd@C_{82}(OH)_{22}]_n$ nanoparticle is a potent activator of dendritic cells and Th1 immune responses. These new findings also provide a rational understanding of the potent anticancer activities of $[Gd@C_{82}(OH)_{22}]_n$ nanoparticles reported previously.

KEYWORDS: nanomedicine · fullerene · dendritic cells · activation · Th1 polarization

Dendritic cells (DCs) serve as a pivotal bridge between innate and adaptive immunity. In peripheral tissues, DCs exist as immature DCs (iDCs). Upon activation following encounter with either exogenous (*e.g.*, pathogen-associated molecular patterns such as microbial nucleic acids, lipopolysaccharides, or flagellin) or endogenous (*e.g.*, CD40 ligand and inflammatory cytokines) stimulators, iDCs undergo a process of activation to become mature DCs (mDCs) that migrate to secondary lymphoid organs for the induction of various immune responses. In the context of antitumor immunity, it has become clear that (1) DCs infiltrate tumor tissues; (2) high levels of more mature DCs in tumor tissues correlate with better clinical outcomes in patients with various cancers, whereas high levels of iDCs in tumor tissues promote tumor progression and inversely correlate with poor prognosis; and (3) DCs loaded with tumor-associated antigens and matured *ex vivo* promote antitumor immune responses in both animal models and human clinical trials.[1] Thus, promotion of DC maturation in tumor-bearing hosts is critical for the induction of antitumor immunity and may provide a novel approach for the development of an effective therapeutic modality for various cancers.

Many kinds of nanomaterials, due to their specific physicochemical properties (*e.g.*, unique sizes and versatile surface functionalizing modifications), are currently under extensive investigation for their potential utilization as drug delivery systems for antitumor chemotherapeutic drugs, as tools for molecular imaging and staging of tumor, or even as therapeutic measures for tumors. Fullerenes and their derivatives belong to a family of widely investigated carbon nanomaterials, which have attracted much attention in recent years due in part to their appealing physical, chemical, and biological properties and to the availabilities of various methods for their surface modification.[2,3] Fullerene derivatives with anti-HIV activity have been synthesized.[2,4−6] Certain hydroxylated/carboxylated fullerenes and fullerene-derivatized amino acids are potent antioxidants. Due to their capacity to scavenge reactive oxygen species (*e.g.*, H_2O_2, $O_2^{\bullet-}$), block apoptosis, and inhibit lipid peroxidation, these fullerene derivatives can be used as neuroprotective agents for the treatment of neurodegenerative disorders (*e.g.*, Parkinson's syndrome, Alzheimer's disease) or to prevent damage caused by ischemia reperfusion.[2,3,7−12] A variety of C_{60} fullerene derivatives show potent antimicrobial activities.[2,13−16] Fullerene derivatives entrapping metal atoms in their carbon cages

*Address correspondence to nzhangchina@yahoo.com.

Received for review October 23, 2009 and accepted January 18, 2010.

Published online February 2, 2010.
10.1021/nn901478z

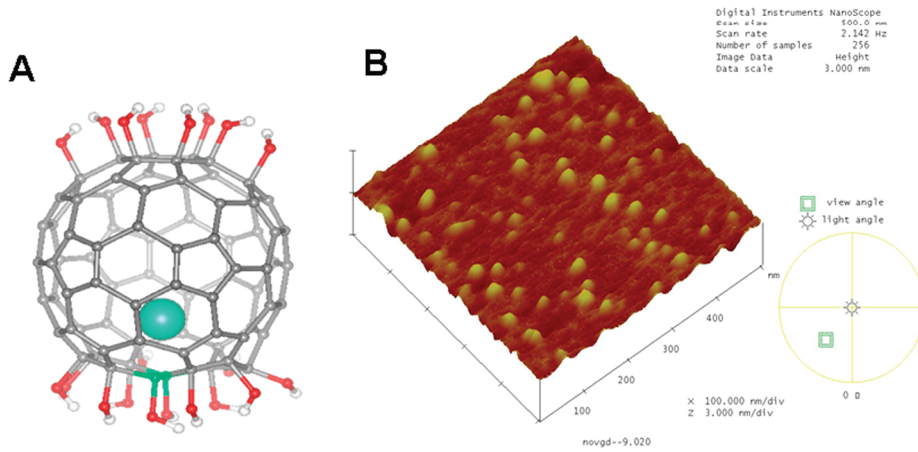

Figure 1. Schematic structure of the Gd@$C_{82}(OH)_{22}$. (A) Schematic structure of the Gd@$C_{82}(OH)_{22}$. (B) AFM image of the $[Gd@C_{82}(OH)_{22}]_n$ nanoparticles.

(metallofullerenes) have been used as radiotracers or contrast agents for X-ray angiography or magnetic resonance imaging (MRI).[17−20]

Gd@$C_{82}(OH)_x$ is a C_{82} fullerene derivative with a gadolinium atom entrapped in the core of the carbon cage while its surface is modified with *x* number of hydroxyl groups. Gd@$C_{82}(OH)_x$ is a water-soluble and biocompatible nanoparticle, which has been studied as a new generation of MRI contrast agent due to its high proton relaxivity.[19] Recently, Gd@$C_{82}(OH)_x$ with $x = 22 \pm 2$ [Gd@$C_{82}(OH)_{22}$] has been synthesized and found to exhibit potent *in vivo* antitumor activity in a mouse hepatoma model.[21] Gd@$C_{82}(OH)_{22}$ in physiologic saline forms molecular aggregates of approximately 22 nm in diameter, hence, it is referred to as a $[Gd@C_{82}(OH)_{22}]_n$ nanoparticle. The antitumor activity of $[Gd@C_{82}(OH)_{22}]_n$ was unlikely due to direct cytotoxic effect since (1) $[Gd@C_{82}(OH)_{22}]_n$ did not directly kill tumor cells, and (2) less than 5% of the intraperitoneally (ip) applied $[Gd@C_{82}(OH)_{22}]_n$ reached the tumor tissue.[21] Interestingly, there was abundant infiltration of leukocytes in the residual tumors of $[Gd@C_{82}(OH)_{22}]_n$-treated mice, whereas no such infiltration was detected in the residual tumors of cyclophosphamide-treated mice.[21] Thus, we propose that $[Gd@C_{82}(OH)_{22}]_n$ may exert its *in vivo* antitumor effect by promoting inflammatory and/or immune response against tumors. To unravel the mechanism by which $[Gd@C_{82}(OH)_{22}]_n$ exerted antitumor effects, we investigated the effect of $[Gd@C_{82}(OH)_{22}]_n$ on DCs and antigen-specific immune responses. The results show that $[Gd@C_{82}(OH)_{22}]_n$ activates myeloid DCs *in vitro* and enhances antigen-specific Th1 immune response *in vivo*, suggesting a novel basis for its potent antitumor activity.

RESULTS AND DISCUSSION

$[Gd@C_{82}(OH)_{22}]_n$ Nanoparticle Induces IL-6 Production by DCs. The schematic structure of the Gd@$C_{82}(OH)_{22}$ is given Figure 1A. The original size of a single Gd@$C_{82}(OH)_{22}$ molecule is less than 2 nm (Figure 1A). However, due to intermolecular interactions, they aggregated into larger particles in saline solution, which was demonstrated by the use of the high-resolution atomic force microscopic (AFM) image technique (Nanoscope system, Digital Instruments Nanoscope, Santa Barbara, CA). The diameters of the $[Gd@C_{82}(OH)_{22}]_n$ aggregates were determined by statistical analysis. The intermolecular aggregation formed $[Gd@C_{82}(OH)_{22}]_n$ particles at 25 nm average, mainly ranging from 10 to 60 nm (Figure 1B).

The antitumor effect of the $[Gd@C_{82}(OH)_{22}]_n$ nanoparticle is accompanied by massive leukocyte infiltration at the sites of residual tumor tissue,[21] suggesting that $[Gd@C_{82}(OH)_{22}]_n$ may promote antitumor immune response. Activation of antigen-presenting cells is the very first step in the induction of any adaptive immune response, so we hypothesized that $[Gd@C_{82}(OH)_{22}]_n$ might have a direct activating effect on DCs, the most potent antigen-presenting cells.[22] As a first step to this end, the effect of $[Gd@C_{82}(OH)_{22}]_n$ on the production of IL-6 by DCs was determined. $[Gd@C_{82}(OH)_{22}]_n$ nanoparticles increased the production of IL-6 by human monocyte-derived DCs in a dose- and time-dependent manner, with more than 35-fold upregulation of IL-6 protein production when DCs were treated with 100 μg/mL of $[Gd@C_{82}(OH)_{22}]_n$ for 48 h (Figure 2A). To identify whether the capacity of $[Gd@C_{82}(OH)_{22}]_n$ preparation to upregulate DC IL-6 production was not due to potential lipopolysaccharide (LPS) contamination, we determined the potential level of LPS in $[Gd@C_{82}(OH)_{22}]_n$ preparation as well as the capacity of polymyxin B (PxB) to block the IL-6-inducing effect of $[Gd@C_{82}(OH)_{22}]_n$ preparation. The LPS level in 1 mg/mL of $[Gd@C_{82}(OH)_{22}]_n$ was below the detection limit of the Limulus Amebocyte Lysate Pyrogen kit (Biowhittaker), suggesting that the $[Gd@C_{82}(OH)_{22}]_n$ preparation used in the present study contained less than 0.6 ng of LPS per mg of $[Gd@C_{82}(OH)_{22}]_n$ (data not shown). Furthermore, DC production of IL-6 was not significantly inhibited by 15 μg/mL of PxB, which, as expected, blocked DC production of IL-6 in response to LPS (Figure 2B).

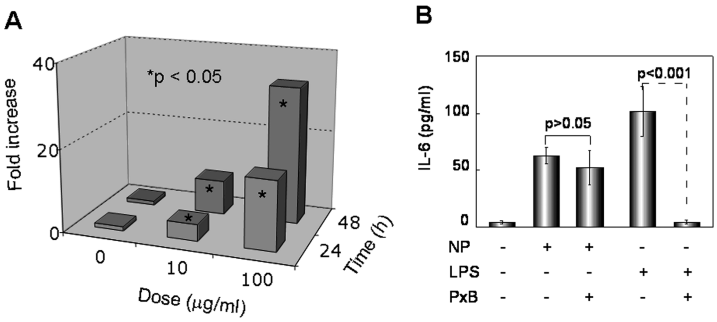

Figure 2. [Gd@$C_{82}(OH)_{22}]_n$ nanoparticle (NP) induction of IL-6 production by DCs. (A) Dose response and time course. Human DCs (5 × 10^5/mL) were incubated at 37 °C in G4 medium in the absence or presence of NP at 10 or 100 μg/mL for 24−48 h, and IL-6 concentrations in the supernatants were measured. The fold increase in DC production of IL-6 was calculated by dividing the background IL-6 concentration (IL-6 in the absence of nanoparticles) by IL-6 concentrations induced by a given concentration of nanoparticles for the same period of time. Shown is the average of three independent experiments when compared with the level of IL-6 in the absence of nanoparticles (*t* test, *$p < 0.05$). (B) Lack of blockade of nanoparticle-induced DC IL-6 by PxB. DCs were incubated in triplicate for 24 h in the presence of nanoparticles (100 μg/mL), LPS (100 ng/mL), and PxB (15 μg/mL), as indicated before the supernatants were collected for IL-6 quantitation. Shown is the average (mean ± SD) IL-6 concentration of triplicate cultures (*p* values were calculated based on *t* test).

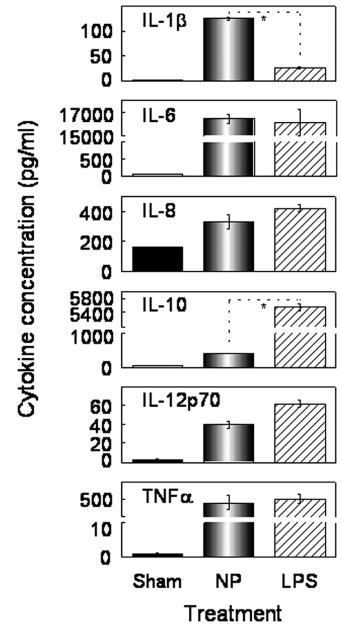

Figure 3. [Gd@$C_{82}(OH)_{22}]_n$ nanoparticle upregulation of multiple DC cytokines. Human DCs (1 × 10^6/mL) were incubated in triplicate at 37 °C in the absence (sham) or presence of 100 μg/mL of nanoparticle or 1 μg/mL of LPS for 48 h. Subsequently, the supernatants were collected for the quantitation of a variety of cytokines as indicated. Shown is the average (mean ± SD) of two independent experiments; *$p <$ 0.05 by *t* test.

Therefore, the capacity of [Gd@$C_{82}(OH)_{22}]_n$ preparation to induce IL-6 production by DCs was not due to LPS contamination.

[Gd@$C_{82}(OH)_{22}]_n$ Nanoparticle Stimulates Phenotypic Maturation of DCs. The capacity of the [Gd@$C_{82}(OH)_{22}]_n$ nanoparticle to induce IL-6 production prompted us to investigate the capacity of [Gd@$C_{82}(OH)_{22}]_n$ to stimulate DC maturation. DC maturation is characterized by three hallmarks: production of a variety of inflammatory cytokines, upregulation of surface costimulatory and MHC molecules, and switch of chemokine responsiveness based on changes in chemokine receptor expression.[22] To examine whether [Gd@$C_{82}(OH)_{22}]_n$ nanoparticles could stimulate DCs to produce cytokines indicative of DC maturation, monocyte-derived DCs were incubated in the presence of [Gd@$C_{82}(OH)_{22}]_n$ (100 μg/mL) or LPS (as a positive control, 1 μg/mL) for 48 h, followed by quantization of cytokine levels in the culture supernatants. As shown by Figure 3, DCs treated with [Gd@$C_{82}(OH)_{22}]_n$ increased this production of IL-1β, IL-6, IL-8, IL-10, IL-12p70, and TNFα. DCs treated with LPS (as a positive control) also upregulated all the above assayed cytokines (Figure 3). However, [Gd@$C_{82}(OH)_{22}]_n$-treated DCs produced significantly more IL-1β and much less IL-10 than LPS-treated DCs (Figure 3).

Cell surface expression of co-stimulatory and MHC molecules by myeloid DC after treatment with the [Gd@$C_{82}(OH)_{22}]_n$ nanoparticle was determined by flow cytometry (Figure 4). Compared with sham-treated DCs (upper panels), LPS-treated DCs became positive for CD83, a marker for DC maturation, and showed enhanced levels of surface CD80, CD86, HLA-ABC, and HLA-DR on their cell surface (Figure 4, lower panels). The [Gd@$C_{82}(OH)_{22}]_n$ nanoparticle promoted the expression of CD83, CD80, CD86, HLA-ABC, and HLA-DR by DCs in a dose-dependent manner (Figure 4, middle panels). Upregulation of CD86, HLA-ABC, and HLA-DR began to occur at as low as 1 μg/mL [Gd@$C_{82}(OH)_{22}]_n$, whereas upregulation of CD83 and CD80 did not become apparent until a higher dose of 100 μg/mL [Gd@$C_{82}(OH)_{22}]_n$ nanoparticle was used.

Immature myeloid DCs express multiple chemokine receptors such as CCR5, which enable them to migrate in response to many inflammatory chemokines such as CCL5, while mature DCs downregulate this receptor and instead upregulate CCR7, a receptor specific for the constitutive chemokines CCL19 and CCL21.[22,23] Upon treatment with LPS, a potent inducer of DC maturation, DC migrated to CCL19 but not CCL5 (Figure 5, hatched bars). DCs treated with the [Gd@$C_{82}(OH)_{22}]_n$ nanoparticle similarly acquired the capacity to migrate to CCL19 and simultaneously lost the responsiveness to CCL5 (Figure 5, dotted bars). Meanwhile, sham-treated DCs migrated to CCL5 but not CCL19, indicative of their immature phenotype (Figure 5, white bars). CXCL12 was used as a positive control because it can induce the migration of both immature and mature DCs. On the basis of the capacity to promote DC production of proinflammatory cytokines (Figure 3) and to upregulate DC surface markers such as CD80, CD83, CD86, HLA-ABC, and HLA-DR (Figure 4), as well as to convert DCs from CCL5 responsive to CCL19 responsive (Figure 5), it can be concluded that the [Gd@$C_{82}(OH)_{22}]_n$ nanoparti-

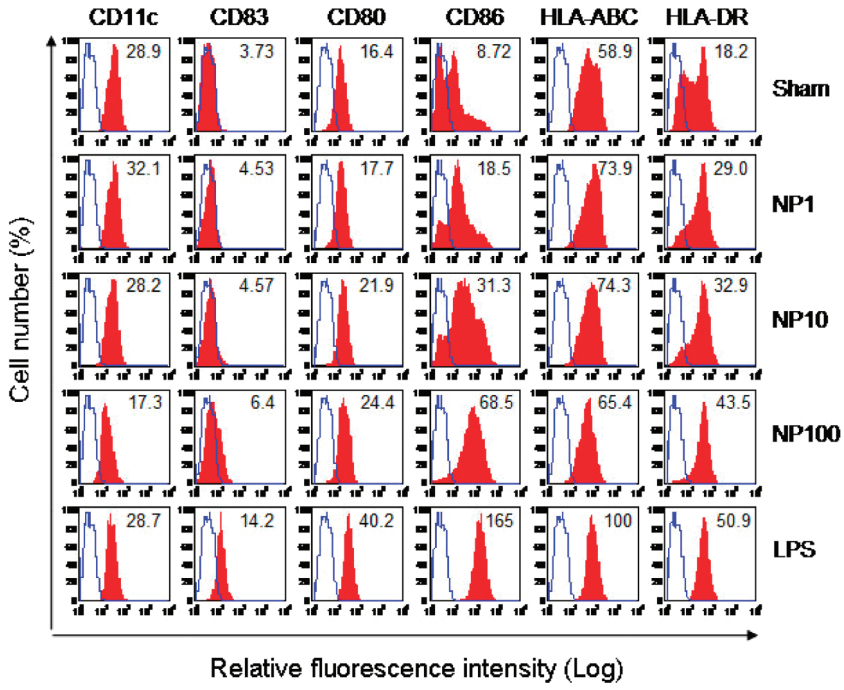

Figure 4. $[Gd@C_{82}(OH)_{22}]_n$ nanoparticle enhancement of surface expression of multiple DC marker molecules. DCs (5×10^5/mL) were incubated at 37 °C for 48 h in the absence (sham) or presence of various concentration (1, 10, 100 μg/mL) of nanoparticle or 1 μg/mL of LPS (as a positive control). Subsequently, the treated DCs were immunostained with a combination of FITC-conjugated antihuman CD83 (FITC-CD83) and PE-conjugated antihuman CD11c (PE-CD11c), FITC-CD80/PE-CD86, or FITC-HLA-ABC/PE-HLA-DR and analyzed by flow cytometry. Shown are the histograms of one experiment representative of three. The blue open area is the relative fluorescence of DCs stained with isotype-matched control antibody; the red closed area is the relative fluorescence intensity of DCs stained with various antibodies. The number inside the histogram is the geometric mean fluorescence intensity of the indicated surface molecule on DCs upon distinct treatment.

cle is capable of inducing the phenotypic maturation of DCs.

$[Gd@C_{82}(OH)_{22}]_n$ Nanoparticle-Matured Human DCs Activate T Cells in a Th1-Polarizing Direction. To determine whether $[Gd@C_{82}(OH)_{22}]_n$ nanoparticle-induced maturation of DCs was reflected at the functional level, $[Gd@C_{82}(OH)_{22}]_n$ nanoparticle-treated DCs were analyzed for their capacity to stimulate the proliferation and activation of T cells in an allogeneic mixed lymphocyte reaction (MLR) setting (Figure 6). Whereas sham-treated DCs did not stimulate the proliferation of allogeneic T cells as judged by their inability to increase

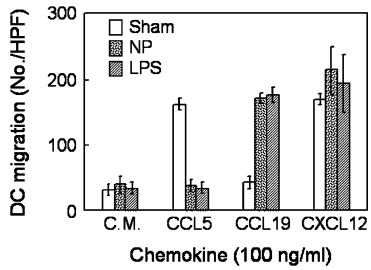

Figure 5. $[Gd@C_{82}(OH)_{22}]_n$ nanoparticle alters DCs' responsiveness to selected chemokines. DCs (1×10^6/mL) were incubated at 37 °C for 48 h in the absence (sham) or presence of NP (100 μg/mL) or LPS (1 μg/mL). Subsequently, treated DCs were harvested and washed, and their capacity to migrate in response to various chemokines (CCL5, CCL19, and CXCL12) was determined using a 48-well microchemotaxis chamber assay as detailed in the Materials and Methods section. Data are the average (mean ± SD) numbers of the migrated DCs of triplicate wells.

tritiated thymidine (^{3}H-TdR) incorporation at any DC/T ratio (Figure 6A, circles), LPS-treated DCs (as a positive control) stimulated considerable proliferation of allogeneic T cells at DC/T ratios higher than 1:6250 (Figure 6A, diamonds). DCs treated with the $[Gd@C_{82}(OH)_{22}]_n$ nanoparticle also stimulated the proliferation of allogeneic T cells in a dose-dependent fashion (Figure 6A, triangles). DCs matured by 10 μg/mL of the $[Gd@C_{82}(OH)_{22}]_n$ nanoparticle began to induce significant proliferation of allogeneic T cells when used at a DC/T ratio higher than 1:250 (Figure 6A, open triangles), while DCs matured by 100 μg/mL of the $[Gd@C_{82}(OH)_{22}]_n$ nanoparticle stimulated significant proliferation of allogeneic T cells at DC/T ratios higher than 1:6250 (Figure 6A, closed triangles). Therefore, $[Gd@C_{82}(OH)_{22}]_n$ nanoparticle-treated DCs exhibited a remarkably enhanced capacity for presenting antigen to T cells for the stimulation of cell proliferation, indicating that the $[Gd@C_{82}(OH)_{22}]_n$ nanoparticle was capable of inducing functional maturation of DCs.

Analysis of the supernatants of day 3 allogeneic MLR for the production of T-cell-derived cytokines showed that $[Gd@C_{82}(OH)_{22}]_n$ nanoparticle-matured DCs in comparison with sham-treated DCs activated allogeneic T cells to produce elevated levels of IL-2, IFNγ, and IL-17 and a decreased level of IL-10, with no significant change in the production of IL-4 (Figure 6B). This profile of T cell cytokines is characteristic of a Th1 re-

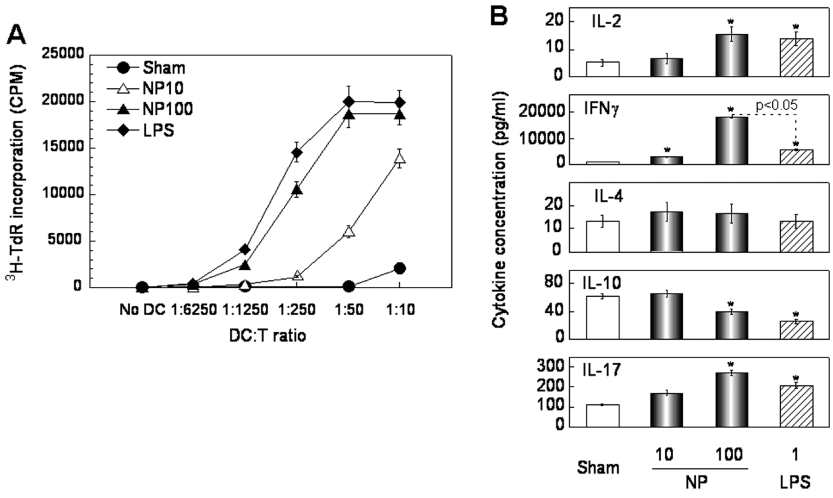

Figure 6. $[Gd@C_{82}(OH)_{22}]_n$ nanoparticle-treated DCs acquire the capacity to stimulate the proliferation and activation of allogeneic T lymphocytes. DCs (5×10^5/mL) were incubated at 37 °C for 48 h in the absence (sham) or presence of NP (10 or 100 μg/mL) or LPS (1 μg/mL). Subsequently, treated DCs were harvested and used for allogeneic MLR. (A) DCs were cocultured in triplicate in wells of a 96-well plate with allogeneic T lymphocyte (10^5/well) at various DC/T ratios for 5 days with the addition of $[^3H]$-TdR in the last 18 h of culture. The cultures were then harvested, and the incorporation of $[^3H]$-TdR was measured by liquid scintillation counting. Shown is the average (mean ± SD) incorporated radioactivity (CPM) of triplicate wells of one experiment representative of three. (B) DCs were mixed with allogeneic T cells (10^6/mL/well) at a DC/T ratio of 1:25 in a 24-well plate and incubated for 3 days before harvesting the supernatants for the quantitation of cytokines. Shown is the average (mean ± SD) cytokine concentration of three independent experiments; *$p < 0.05$ compared with the level of T cell cytokine in response to sham-treated DCs.

sponse. The Th1-polarizing effect of the $[Gd@C_{82}(OH)_{22}]_n$ nanoparticle was dose-dependent: the higher the concentration of the $[Gd@C_{82}(OH)_{22}]_n$ nanoparticle used for the treatment of DCs, the greater the effect of the $[Gd@C_{82}(OH)_{22}]_n$-treated DCs on the production of T-cell-derived cytokines (Figure 6B). LPS-matured DCs, as expected, activated allogeneic T cells to generate elevated levels of IL-2, IFNγ, and IL-17 as well as a decreased level of IL-10, with no significant change in the production of IL-4 (Figure 6B) because LPS is a known Th1-polarizing DC activator. Strikingly, $[Gd@C_{82}(OH)_{22}]_n$-matured DCs induced greater IFNγ production than LPS-matured DCs by allogeneic T cells, indicating that the $[Gd@C_{82}(OH)_{22}]_n$ nanoparticle may be a more efficacious Th1-polarizing DC activator than LPS (Figure 6B).

$[Gd@C_{82}(OH)_{22}]_n$ Nanoparticle-Enhanced Antigen-Specific Th1 Immune Response *In Vivo*. Th1 immune response plays an essential role in antitumor immunotherapies. The capability of the $[Gd@C_{82}(OH)_{22}]_n$ nanoparticle to mature DCs in a Th1-polarizing direction suggested that it might act as an immunoenhancer for the promotion of *in vivo* antigen-specific Th1 immune response. To validate this possibility, C57BL/6 mice were immunized with ovalbumin (OVA) in the absence or presence of the $[Gd@C_{82}(OH)_{22}]_n$ nanoparticle or alum (as a positive control) on day 0 and boosted with OVA alone on day 14; their spleens were removed on day 21 for the determination of OVA-specific proliferation and cytokine production. As expected, splenocytes from mice immunized with OVA in the presence of alum incorporated significantly more ^{3}H-TdR than cells of mice immunized with OVA alone (PBS group), particularly when the concentration of OVA used for *in vitro* stimulation reached 50 μg/mL (Figure 6A). Importantly, splenocytes of mice immunized with OVA in the presence of $[Gd@C_{82}(OH)_{22}]_n$ nanoparticles also showed enhanced proliferation upon *in vitro* stimulation with OVA (Figure 7A), indicating enhancement of mouse anti-OVA immune response by the $[Gd@C_{82}(OH)_{22}]_n$ nanoparticle. Upon stimulation with OVA, splenocytes of mice immunized with OVA plus $[Gd@C_{82}(OH)_{22}]_n$ nanoparticle produced predominantly Th1 cytokines, namely, IFNγ, without upregulation of Th2 cytokines (*e.g.*, IL-4, IL-5, and IL-10). The splenocytes of mice immunized with OVA plus $[Gd@C_{82}(OH)_{22}]_n$ nanoparticle also produced higher levels of IL-1β and IL-2 than those of mice immunized with OVA alone (Figure 7B). Therefore, $[Gd@C_{82}(OH)_{22}]_n$ nanoparticle demonstrated the capacity to promote *in vivo* antigen-specific Th1-type T cell response (Figure 7B). Alum, as expected, enhanced predominantly Th2 responses as evidenced by upregulation of indicator cytokines such as IL-4, IL-5, and IL-10 (Figure 7B).

$Gd@C_{82}(OH)_{22}$ has been developed as a potent and novel antitumor agent without detectable cytotoxicity *in vitro* or toxic side effects in mouse models. However, the molecular mechanism of $Gd@C_{82}(OH)_{22}$-induced antitumor activities is largely unknown. Our previous studies revealed that intraperitoneal administration of the $[Gd@C_{82}(OH)_{22}]_n$ nanoparticle caused a remarkable inhibition of the growth of subcutaneously implanted mouse hepatoma tumor, which was accompanied by marked infiltration of leukocytes in residual tumor tissue.[21] Since leukocyte infiltration of tumor tissues is often indicative of inflammatory and/or immune responses against tumor, this suggests that $[Gd@C_{82}(OH)_{22}]_n$ may activate DCs, which promotes both inflammatory and immune responses.[22] Incubation of human DCs with $[Gd@C_{82}(OH)_{22}]_n$ resulted in both phenotypic and functional maturation of DCs as evidenced by the acquisition of numerous hallmarks of DC maturation (production of proinflammatory cytokines, upregulation of surface expression of costimulatory and MHC molecules, and switch from CCL19 unresponsive to CCL19 responsive), as well as the capacity to present antigen to naïve T cells (Figures 2−6A). Analysis of the cytokine profiles generated by activated T cells in response to $[Gd@C_{82}(OH)_{22}]_n$-treated DCs revealed a predominant upregulation of IFNγ and IL-17 but not of IL-4 or IL-10, suggesting that

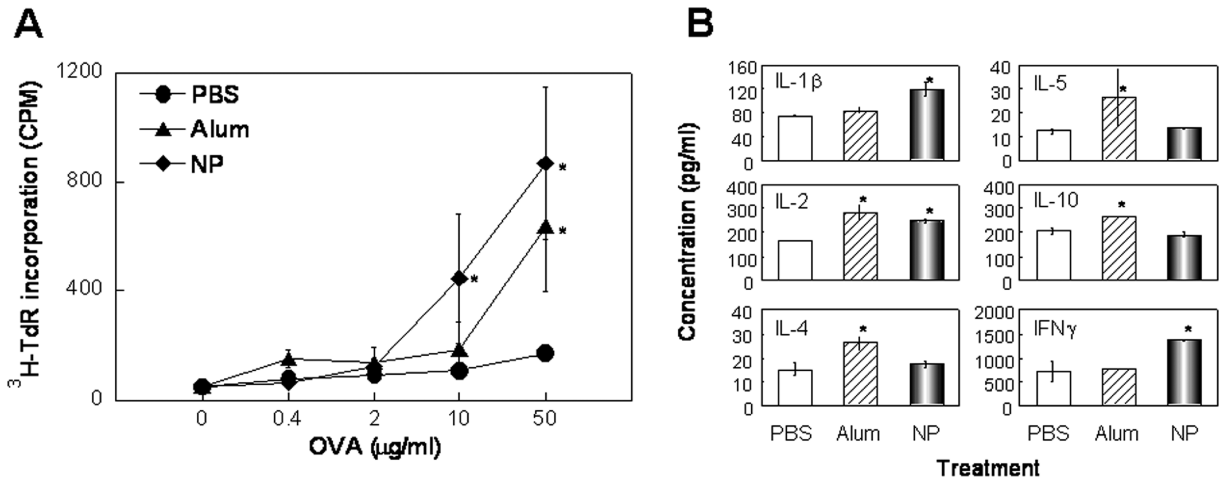

Figure 7. $[Gd@C_{82}(OH)_{22}]_n$ nanoparticle enhancement of antigen-specific immune response. C56BL/6 mice ($n = 4$) were ip immunized with OVA (50 μg/mouse) in the absence or presence of nanoparticle (10 μg/mouse) or alum (as a positive control) on day 1, boosted ip with OVA alone on day 14, and euthanized on day 21 for the preparation of single splenocyte suspension. (A) OVA-specific proliferation of splenocytes. Splenocytes were cultured in triplicate in a 96-well plate at 2×10^5/well in the presence of various concentrations of OVA for 60 h and pulsed with 0.5 μCi/well of [^{3}H]-TdR for the last 18 h. Proliferation of splenocytes was measured as [^{3}H-TdR] incorporation and shown as the average (mean ± SD) incorporated radioactivity (CPM) of four mice; *$p < 0.05$ compared with the corresponding PBS group (immunized with OVA alone). (B) Pooled splenocytes of each group were cultured in duplicate in a 24-well plate at 5×10^6/1 mL/well in RPMI 1640 containing 10% FBS and 50 μg/mL of OVA for 48 h before harvesting the supernatants for cytokine measurement. Shown is the average (mean ± SD) cytokine concentration of four mice. Similar results were obtained in two independent experiments; *$p < 0.05$ compared with the PBS group.

$[Gd@C_{82}(OH)_{22}]_n$ has the capacity to induce a Th1-polarized immune response (Figure 6B). This notion was validated *in vivo* because immunization of mice with a mixture of an antigen (OVA) and $[Gd@C_{82}(OH)_{22}]_n$ resulted in the generation of OVA-specific Th1-polarized immune response (Figure 7). The immunoenhancing adjuvant effect of $[Gd@C_{82}(OH)_{22}]_n$ is in distinct contrast to that of alum, which predominantly promotes antigen-specific Th2 response as indicated by enhancement of IL-4, IL-5, and IL-10 but not of IFNγ (Figure 7B). The Th2-enhancing adjuvant effect of alum is well-documented.[24] Therefore, the results demonstrate that $[Gd@C_{82}(OH)_{22}]_n$ can activate DCs and promote Th1-type immune response, which may account for, at least in part, its antitumor activities.

Although the data of the current study demonstrate that $[Gd@C_{82}(OH)_{22}]_n$ can induce full maturation of DCs as indicated by the induction of many cytokines (Figures 1 and 2), upregulation of surface co-stimulatory and MHC molecules (Figure 3), and switch of chemokine responsiveness (Figure 4), how $[Gd@C_{82}(OH)_{22}]_n$ exerts its effect on DCs remains to be investigated. The DC-maturing effect of $[Gd@C_{82}(OH)_{22}]_n$ is unlikely due to contamination by LPS because (1) the $[Gd@C_{82}(OH)_{22}]_n$ preparation used in the present study did not contain a detectable level of LPS and (2) its IL-6-inducing effect could not be blocked by PxB, a widely used LPS-neutralizing reagent (Figure 1B). Furthermore, the profile of DC cytokines induced by $[Gd@C_{82}(OH)_{22}]_n$ is clearly different from that induced by LPS (Figure 2): $[Gd@C_{82}(OH)_{22}]_n$ induced much more IL-1β and much less immunosuppressive IL-10 than LPS. This difference not only indicates that the DC-activating effect of $[Gd@C_{82}(OH)_{22}]_n$ is unlikely due to LPS contamination but also suggests that $[Gd@C_{82}(OH)_{22}]_n$ may be even more efficacious than LPS at enhancing immune responses. Our preliminary attempt to study the interaction between $[Gd@C_{82}(OH)_{22}]_n$ and DCs revealed that, upon addition to DC culture *in vitro*, $[Gd@C_{82}(OH)_{22}]_n$ was rapidly engulfed by DCs (data not shown). However, engulfment of inert particles (*e.g.*, latex beads and dextran, *etc.*) by DCs *per se* generally does not generally cause DC maturation. In contrast, a multihydroxylated C_{60} fullerene nanoparticle without a Gd atom, $[C_{60}(OH)_{26}]_n$, also exhibited the capacity to induce DC activation *in vitro*, albeit less potent than $[Gd@C_{82}(OH)_{22}]_n$, suggesting that Gd may not be required for activating DCs (data not shown). C_{60} or C_{82} fullerenes without hydroxylation were not water-soluble hence could not be tested in our assays. Therefore, the DC-activating effect of $[Gd@C_{82}(OH)_{22}]_n$ is likely based on its unique properties in aqueous solution, including its size and multiple hydroxylation.

$[Gd@C_{82}(OH)_{22}]_n$ is the first fullerene-derived nanoparticle shown to promote both DC maturation and antigen-specific immune response (Scheme 1). Several nanoformulations have recently been reported to have the capacity to induce the maturation of dendritic cells and/or to promote immune responses, such as very small size proteoliposome, monophosphoryl lipid A containing copolymer, poly(γ-glutamic acid) nanoparticles, or polystyrene beads.[25−28] However, most of these nanoparticle-induced responses were due to microbial components attached to the nanoparticles (namely, Neisserial outer membrane protein and lipid A derivative, respectively).[25,26] $[Gd@C_{82}(OH)_{22}]_n$ is quite unique

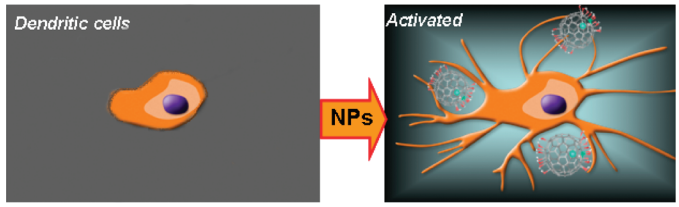

Scheme 1.

since it selectively enhances antigen-specific Th1 response, whereas polystyrene microbeads and (γ-glutamic acid) nanoparticles are capable of enhancing both Th1 and Th2 immune responses.[27−29] Induction of the Th1-type of tumor antigen-specific immune response (*e.g.*, IFNγ and CD8 T cells) is more effective in achieving therapeutic antitumor responses, so $[Gd@C_{82}(OH)_{22}]_n$ may prove to be a good candidate for potential antitumor therapeutic implication.

The *in vivo* antitumor activity of $[Gd@C_{82}(OH)_{22}]_n$ is based on more than just promoting the activation of DCs and antitumor immunity. $[Gd@C_{82}(OH)_{22}]_n$ reduces oxidative stress in tumor-bearing mice, which may contribute to its antitumor activity because oxidative stress can promote tumor progression.[30] In a preliminary study, we observed that administration of $[Gd@C_{82}(OH)_{22}]_n$ to tumor-bearing mice reduced the blood supply into tumor tissues (data not shown). Limiting blood supply to the tumor tissue by $[Gd@C_{82}(OH)_{22}]_n$ may also contribute to its antitumor activity by inhibiting tumor growth. Thus, the *in vivo* antitumor activity of $[Gd@C_{82}(OH)_{22}]_n$ is most likely mediated by its effects on promoting DC activation, reducing oxidative stress, and reducing blood supply to tumor tissues.

CONCLUSION

$[Gd@C_{82}(OH)_{22}]_n$ possesses novel properties that make this reagent a promising drug candidate, capable of simultaneously enabling tumor detection, treatment, and evaluation of therapeutic efficacy. First, $[Gd@C_{82}(OH)_{22}]_n$ exhibits good biocompatibility, stability, and no obvious toxic side effect both *in vitro* and *in vivo*.[12,21] Second, it shows potent *in vivo* antitumor activity.[21] Furthermore, due to the entrapment of a gadolinium atom, it can be potentially used as a good contrast reagent in the detection, staging, and/or monitoring of tumors based on MRI.[3,19−21] Our study's results suggest that the $Gd@C_{82}(OH)_{22}$ nanoparticle may promote antitumor immune response in tumor-bearing hosts. Thus, $Gd@C_{82}(OH)_{22}$ nanoparticles, due to their unique physical size, surface chemical properties, and capacity of simultaneously targeting multiple processes in tumor development, appear to be a promising base for the development of potentially more effective measures for the diagnosis and/or treatment of tumors.

MATERIALS AND METHODS

Reagents and Mice. Recombinant human granulocyte−macrophage colony stimulating factor (GM-CSF, specific activity $\geq 10^7$ U/mg), interleukin-4 (IL-4, specific activity $\geq 2 \times 10^6$ U/mg), stromal cell-derived factor alpha (CXCL12/SDF-1α) regulated on activation and normal T cell expressed (CCL5/RANTES), and secondary lymphoid organ chemokine (CCL19/ELC) were obtained from PeproTech (Rocky Hill, NJ). BSA, OVA, PxB, and LPS (*Escherichia coli*, serotype O55:B5) were from Sigma (St. Louis, MO). Tritiated thymidine (^{3}H-TdR, specific radioactivity = 2 Ci/mmol) was purchased from NEN (Boston, MA). RPMI 1640, glutamine, penicillin, streptomycin, HEPES, and phosphate-buffered saline (PBS, pH = 7.4) were from Biowhittaker (Walkersville, MD). Fetal bovine serum (FBS) was purchased from Hyclone (Logan, UT). All antibodies used for flow cytometry analysis were purchased from BD/PharMingen (San Diego, CA), including FITC-conjugated mouse antihuman CD83 (IgG1, κ, clone HB15e), FITC-conjugated mouse antihuman CD80 (IgG1, κ, clone L307.4), FITC-conjugated mouse antihuman HLA-ABC (IgG1, κ, clone G46-2.6), phycoerythrin (PE)-conjugated mouse antihuman CD11c (IgG1, clone B-Ly6), PE-conjugated mouse antihuman CD86 (IgG1, κ, clone 2331), PE-conjugated mouse antihuman HLA-DR (IgG2a, κ, clone G46-6), and FITC- and/or PE-conjugated isotype-matched mouse IgG controls (IgG1, κ and IgG2a, κ). QCL-1000 chromogenic LAL assay kit was purchased from Cambrex (Walkersville, MD).

C57BL/6 mice (6−7 weeks old) were purchased from Charles River (Frederick, MD) and allowed to acclimate for at least 2 weeks before experimental use. All mice were kept under specific pathogen-free condition with water and food given *ad libitum*. Mouse care and use were in compliance with the principles and procedures outlined in the NIH Guide for the Care and Use of Animals.

Preparation and Characterization of the $[Gd@C_{82}(OH)_{22}]_n$ Nanoparticles. The $Gd@C_{82}$ was synthesized by the arc-discharge method using composite rods consisting of Gd_2O_3 (purity >99.99%) and graphite (purity >99.99%) in He atmosphere. The separation of $Gd@C_{82}$ was performed by a two-step high-performance liquid chromatography (HPLC, LC908-C60, Japan Analytical Industry Co.), and the details were reported previously.[31,32] The purity of the final $Gd@C_{82}$ product was >99.5%. $Gd@C_{82}(OH)_{22}$ was synthesized by the alkaline reaction, the same as reported elsewhere.[21,30,33] The MALDI-TOF-MS technique (AutoFlex, Bruker Co., Germany), X-ray photoemission spectroscopy (XPS, Beijing Synchrotron Radiation Facility), and element analyses were employed to measure surface hydroxyl groups. $[Gd@C_{82}(OH)_{22}]_n$ was dissolved in endotoxin-free water to make a stock solution of 10 mg/mL and kept at 4 °C until use. The schematic structure of the $Gd@C_{82}(OH)_{22}$ is given in Figure 1A, and Figure 1B shows the AFM image of the $[Gd@C_{82}(OH)_{22}]_n$ nanoparticles. The average particle size is about 25 nm, mainly ranging from 10 to 60 nm.

Isolation and Purification of Cells. Human peripheral blood mononuclear cells (PBMCs) were isolated by Ficoll density gradient centrifugation from leukopacks supplied by the Department of Transfusion Medicine (Clinical Center, National Institute of Health, Bethesda, MD).[9] Monocytes were purified (>95%) from human PBMC with MACS CD14 monocyte isolation kit (Miltenyi Biotech Inc., Auburn, CA). Human peripheral blood T cells were isolated from human PBMC by using a CD3 enrichment column (R&D System) following the manufacturer's instruction.

DC Culture. DCs were generated as described previously.[9] In brief, monocyte-derived immature DCs (Mo-iDCs) were generated by incubating purified peripheral blood monocytes at 2−5 $\times 10^5$/mL in G4 medium (RPMI 1640 containing 10% FBS, 2 mM glutamine, 25 mM HEPES, 100 U/mL penicillin, 100 μg/mL streptomycin, 50 ng/mL GM-CSF, and 50 ng/mL IL-4) at 37 °C in a CO_2 (5%) incubator for 5−6 days. Subsequently, DCs were incubated at 5−10 $\times 10^5$/mL in fresh G4 medium in the absence or presence of $[Gd@C_{82}(OH)_{22}]_n$ nanoparticle or LPS at specified concentrations for 24−48 h in a CO_2 (5%) incubator before analysis

of their production of cytokines, expression of surface markers, and capability of antigen presentation. In some experiments, PxB was added to DC cultures at a final concentration of 10−15 μg/mL.

Cytokine Quantitation. The cytokines (IL-1β, IL-2, IL-4, IL-5, IL-6, IL-8, IL-10, IL-12p70, IL-17, TNFα, and IFNγ) in the supernatants of cultured human and mouse cells were quantitated using a SearchLight Multiplex Proteome Array (Pierce Biotech, Woburn, MA).

Flow Stain and Analysis. DCs (10^6/sample) were first washed three times with FACS buffer (PBS, 1% FBS, 0.02% NaN_3, pH 7.4). After blocking for 15 min at 4 °C in FACS buffer containing 1% human AB serum and 1% normal mouse serum, DCs were incubated with various FITC- or PE- conjugated mouse monoclonal antibodies against human CD11c, CD80, CD83, CD86, HLA-ABC, HLA-DR, or isotype-matched control antibody at 4 °C for 30 min as specified. Subsequently, the cells were washed (twice with FACS buffer and twice with PBS), suspended in PBS, and analyzed with a Becton-Dickinson FACScan cytometer.

DC Migration Assay. DC migration in response to chemokines was determined using a 48-well microchemotaxis chamber assay as previously described.[9] In brief, chemokines (100 ng/mL) and DCs (10^6/mL) in chemotaxis medium (C.M., RPMI 1640 containing 1% BSA) were put into the lower and upper wells, respectively, of a 48-well microchemotaxis chamber (Neuro Probe, Cabin John, MA), with the lower and upper compartments separated by a 5 μM polycarbonate filter (Osmonics, Livermore, CA). After incubation at 37 °C for 1.5 h in humidified air with 5% CO_2, the filters were removed and stained, and the cells migrated across the filter were counted with the use of a Bioquant semiautomatic counting system (Bioquant Image Analysis Corp, Nashville, TN). The results were presented as the number of cells per high power field (No./HPF).

Mixed Lymphocyte Reaction (MLR). Allogeneic MLR was performed as described.[9] Briefly, purified human allogeneic T cells (10^5/well) were cultured with different numbers of DCs in a 96-well flat-bottom plate for 6 days at 37 °C in humidified air with 5% CO_2. The proliferative response of T cells was examined by pulsing the culture with ^{3}H-TdR (0.5 μCi/well) for the last 18 h before cell harvest. ^{3}H-TdR incorporation was measured with a microbeta counter (Wallac, Gaithersburg, MD). Alternatively, the supernatants of the MLR cultures were collected for cytokine quantitation.

Immunization and Detection of Antigen-Specific Immune Responses. Eight-week-old C57BL/6 mice (3−5 mice/group) were injected i.p. on day 1 with 0.2 mL of PBS containing either 50 μg of OVA (Sigma), or a mixture of 50 μg of OVA and 10 μg of $[Gd@C_{82}(OH)_{22}]_n$ nanoparticle, or 50 μg of OVA absorbed onto 3 mg of alum (Sigma). On day 14, all mice were booster immunized by ip injection of 0.2 mL of PBS containing 50 μg of OVA. On day 21, immunized mice were euthanized to remove spleens and to make single splenocyte suspension. OVA-specific splenocyte proliferation and/or cytokine production was measured as previously described with minor modifications.[34] Briefly, splenocytes (2×10^5/well) were seeded in triplicate in wells of round-bottomed 96-well plates in complete RPMI 1640 medium (0.2 mL/well) and incubated in the presence or absence of an indicated concentration of OVA at 37 °C in a CO_2 incubator for 60 h. The cultures were pulsed with ^{3}H-TdR (1 μCi/well) for the last 18 h for the measurement of splenocyte proliferation. Alternatively, splenocytes were cultured in duplicate in complete RPMI1640 in 24-well plates (5×10^6/1 mL/well) having indicated concentrations of OVA for 48 h before the culture supernatants were harvested for cytokine quantitation.

Acknowledgment. This project has been funded in part with Federal funds from the National Cancer Institute, National Institutes of Health, under Contract No. NO1-CO-12400. The content of this publication does not necessarily reflect the views or policies of the Department of Health and Human Services, nor does mention of trade names, commercial products, or organizations imply endorsement by the U.S. Government. The project was also funded in part by NSFC (30772529), China MOST 973 projects (2010CB933900), Tianjin Commission of Science and Technology(08ZCKFSH04800) CAS knowledge innovation program, and U.S. National Foundation of Cancer Research.

REFERENCES AND NOTES

1. Chaput, N.; Conforti, R.; Viaud, S.; Spatz, A.; Zitvogel, L. The Janus Face of Dedritic Cells in Cancer. *Oncogene* **2008**, *27*, 5920–5931.
2. Bosi, S.; Da Ros, T.; Spalluto, G.; Prato, M. Fullerene Derivatives: An Attractive Tool for Biological Applications. *Eur. J. Med. Chem.* **2003**, *38*, 913–923.
3. Tang, J.; Xing, G.; Zhao, F.; Yuan, H.; Zhao, Y. Modulation of Structural and Electronic Properties of Fullerene and Metallofullerenes by Surface Chemical Modifications. *J. Nanosci. Nanotechnol.* **2007**, *7*, 1085–1101.
4. Schinazi, R. F.; Sijbesma, R.; Srdanov, G.; Hill, C. L.; Wudl, F. Synthesis and Virucidal Activity of a Water-Soluble, Configurationally Stable, Derivatized C60 Fullerene. *Antimicrob. Agents Chemother.* **1993**, *37*, 1707–1710.
5. Friedman, S. H.; Ganapathi, P. S.; Rubin, Y.; Kenyon, G. L. Optimizing the Binding of Fullerene Inhibitors of the HIV-1 Protease through Predicted Increases in Hydrophobic Desolvation. *J. Med. Chem.* **1998**, *41*, 2424–2429.
6. Mashino, T.; Shimotohno, K.; Ikegami, N.; Nishikawa, D.; Okuda, K.; Takahashi, K.; Nakamura, S.; Mochizuki, M. Human Immunodeficiency Virus—Reverse Transcriptase Inhibition and Hepatitis C Virus RNA-Dependent RNA Polymerase Inhibition Activities of Fullerene Derivatives. *Bioorg. Med. Chem. Lett.* **2005**, *15*, 1107–1109.
7. Dugan, L. L.; Gabrielsen, J. K.; Yu, S. P.; Lin, T. S.; Choi, D. W. Buckminsterfullerenol Free Radical Scavengers Reduce Excitotoxic and Apoptotic Death of Cultured Cortical Neurons. *Neurobiol. Dis.* **1996**, *3*, 129–135.
8. Dugan, L. L.; Lovett, E. G.; Quick, K. L.; Lotharius, J.; Lin, T. T.; O'Malley, K. L. Fullerene-Based Antioxidants and Neurodegenerative Disorders. *Parkinsons Relat. Disord.* **2001**, *7*, 243–246.
9. Laakkonen, P.; Akerman, M. E.; Biliran, H.; Yang, M.; Ferrer, F.; Karpanen, T.; Hoffman, R. M.; Ruoslahti, E. Antitumor Activity of a Homing Peptide that Targets Tumor Lymphatics and Tumor Cells. *Proc. Natl. Acad. Sci. U.S.A.* **2004**, *101*, 9381–9386.
10. Fumelli, C.; Marconi, A.; Salvioli, S.; Straface, E.; Malorni, W.; Offidani, A. M.; Pellicciari, R.; Schettini, G.; Giannetti, A.; Monti, D.; Franceschi, C.; Pincelli, C. Carboxyfullerenes Protect Human Keratinocytes from Ultraviolet-B-Induced Apoptosis. *J. Invest. Dermatol.* **2000**, *115*, 835–841.
11. Pantarotto, D.; Tagmatarchis, N.; Bianco, A.; Prato, M. Synthesis and Biological Properties of Fullerene-Containing Amino Acids and Peptides. *Mini-Rev. Med. Chem.* **2004**, *4*, 805–814.
12. Chen, Y. B.; Jiang, C. T.; Zhang, G. Q.; Wang, J. S.; Pang, D. Increased Expression of Hyaluronic Acid Binding Protein 1 Is Correlated with Poor Prognosis in Patients with Breast Cancer. *J. Surg. Oncol.* **2009**, *100*, 382–386.
13. Mashino, T.; Okuda, K.; Hirota, T.; Hirobe, M.; Nagano, T.; Mochizuki, M. Inhibition of *E. coli* Growth by Fullerene Derivatives and Inhibition Mechanism. *Bioorg. Med. Chem. Lett.* **1999**, *9*, 2959–2962.
14. Tsao, N.; Luh, T. Y.; Chou, C. K.; Wu, J. J.; Lin, Y. S.; Lei, H. Y. Inhibition of Group A Streptococcus Infection by Carboxyfullerene. *Antimicrob. Agents Chemother.* **2001**, *45*, 1788–1793.
15. Tegos, G. P.; Demidova, T. N.; Arcila-Lopez, D.; Lee, H.; Wharton, T.; Gali, H.; Hamblin, M. R. Cationic Fullerenes Are Effective and Selective Antimicrobial Photosensitizers. *Chem. Biol.* **2005**, *12*, 1127–1135.
16. Bianco, A.; Da Ros, T.; Prato, M.; Toniolo, C. Fullerene-Based Amino Acids and Peptides. *J. Pept. Sci.* **2001**, *7*, 208–219.
17. Wharton, T.; Wilson, L. J. Highly-Iodinated Fullerene as a Contrast Agent for X-ray Imaging. *Bioorg. Med. Chem.* **2002**, *10*, 3545–3554.
18. Cagle, D. W.; Kennel, S. J.; Mirzadeh, S.; Alford, J. M.; Wilson, L. J. *In Vivo* Studies of Fullerene-Based Materials Using Endohedral Metallofullerene Radiotracers. *Proc. Natl. Acad. Sci. U.S.A.* **1999**, *96*, 5182–5187.

19. Mikawa, M.; Kato, H.; Okumura, M.; Narazaki, M.; Kanazawa, Y.; Miwa, N.; Shinohara, H. Paramagnetic Water-Soluble Metallofullerenes Having the Highest Relaxivity for MRI Contrast Agents. *Bioconjugate Chem.* **2001**, *12*, 510–514.
20. Bolskar, R. D.; Benedetto, A. F.; Husebo, L. O.; Price, R. E.; Jackson, E. F.; Wallace, S.; Wilson, L. J.; Alford, J. M. First Soluble M@C60 Derivatives Provide Enhanced Access to Metallofullerenes and Permit *In Vivo* Evaluation of $Gd@C_{60}[C(COOH)_2]_{10}$ as a MRI Contrast Agent. *J. Am. Chem. Soc.* **2003**, *125*, 5471–5478.
21. Chen, C.; Xing, G.; Wang, J.; Zhao, Y.; Li, B.; Tang, J.; Jia, G.; Wang, T.; Sun, J.; Xing, L.; Yuan, H.; Gao, Y.; Meng, H.; Chen, Z.; Zhao, F.; Chai, Z.; Fang, X. Multihydroxylated $[Gd@C_{82}(OH)_{22}]_n$ Nanoparticles: Antineoplastic Activity of High Efficiency and Low Toxicity. *Nano Lett.* **2005**, *5*, 2050–2057.
22. Banchereau, J.; Briere, F.; Caux, C.; Davoust, J.; Lebecque, S.; Liu, Y. J.; Pulendran, B.; Palucka, K. Immunobiology of Dendritic Cells. *Annu. Rev. Immunol.* **2000**, *18*, 767–811.
23. Sozzani, S.; Luini, W.; Borsatti, A.; Polentarutti, N.; Zhou, D.; Piemonti, L.; D'Amico, G.; Power, C. A.; Wells, T. N. C.; Gobbi, M.; Allavena, P.; Mantovani, A. Receptor Expression and Responsiveness of Human Dendritic Cells to a Defined Set of CC and CXC Chemokines. *J. Immunol.* **1997**, *159*, 1993–2000.
24. Sugai, T.; Mori, M.; Nakazawa, M.; Ichino, M.; Naruto, T.; Kobayashi, N.; Kobayashi, Y.; Minami, M.; Yokota, S. A CpG-Containing Oligodeoxynucleotide as an Efficient Adjuvant Counterbalancing the Th1/Th2 Immune Response in Diphtheria-Tetanus-Pertussis Vaccine. *Vaccine* **2005**, *23*, 5450–5456.
25. Mesa, C.; De Leon, J.; Rigley, K.; Fernandez, L. E. Very Small Size Proteoliposomes Derived from *Neisseria meningitidis*: An Effective Adjuvant for Th1 Induction and Dendritic Cell Activation. *Vaccine* **2004**, *22*, 3045–3052.
26. Elamanchili, P.; Diwan, M.; Cao, M.; Samuel, J. Characterization of Poly($_{D,L}$-lactic-*co*-glycolic acid) Based Nanoparticulate System for Enhanced Delivery of Antigens to Dendritic Cells. *Vaccine* **2004**, *22*, 2406–2412.
27. Uto, T.; Wang, X.; Sato, K.; Haraguchi, M.; Akagi, T.; Akashi, M.; Baba, M. Targeting of Antigen to Dendritic Cells with Poly(gamma-glutamic acid) Nanoparticles Induces Antigen-Specific Humoral and Cellular Immunity. *J. Immunol.* **2007**, *178*, 2979–2986.
28. Mottram, P. L.; Leong, D.; Crimeen-Irwin, B.; Gloster, S.; Xiang, S. D.; Meanger, J.; Ghildyal, R.; Vardaxis, N.; Plebanski, M. Type 1 and 2 Immunity Following Vaccination Is Influenced by Nanoparticle Size: Formulation of a Model Vaccine for Respiratory Syncytial Virus. *Mol. Pharmaceutics* **2007**, *4*, 73–84.
29. Fifis, T.; Gamvrellis, A.; Crimeen-Irwin, B.; Pietersz, G. A.; Li, J.; Mottram, P. L.; McKenzie, I. F.; Plebanski, M. Size-Dependent Immunogenicity: Therapeutic and Protective Properties of Nano-vaccines against Tumors. *J. Immunol.* **2004**, *173*, 3148–3154.
30. Wang, J.; Chen, C.; Li, B.; Yu, H.; Zhao, Y.; Sun, J.; Li, Y.; Xing, G.; Yuan, H.; Tang, J.; Chen, Z.; Meng, H.; Gao, Y.; Ye, C.; Chai, Z.; Zhu, C.; Ma, B.; Fang, X.; Wan, L. Antioxidative Function and Biodistribution of $[Gd@C_{82}(OH)_{22}]_n$ Nanoparticles in Tumor-Bearing Mice. *Biochem. Pharmacol.* **2006**, *71*, 872–881.
31. Akasaka, T.; Kono, T.; Takematsu, Y.; Nikawa, H.; Nakahodo, T.; Wakahara, T.; Ishitsuka, M. O.; Tsuchiya, T.; Maeda, Y.; Liu, M. T.; Yoza, K.; Kato, T.; Yamamoto, K.; Mizorogi, N.; Slanina, Z.; Nagase, S. Does $Gd@C_{82}$ Have an Anomalous Endohedral Structure? Synthesis and Single Crystal X-ray Structure of the Carbene Adduct. *J. Am. Chem. Soc.* **2008**, *130*, 12840–12841.
32. Wang, L.; Yang, D. Comment on "Electronic Transport, Structure, and Energetics of Endohedral $Gd@C_{82}$ Metallofullerenes. *Nano Lett.* **2005**, *5*, 2340.
33. Liu, Y.; Jiao, F.; Qiu, Y.; Li, W.; Lao, F.; Zhou, G.; Sun, B.; Xing, G.; Dong, J.; Zhao, Y.; Chai, Z.; Chen, C. The Effect of $Gd@C_{82}(OH)_{22}$ Nanoparticles on the Eelease of Th1/Th2 Cytokines and Induction of TNF-alpha Mediated Cellular Immunity. *Biomaterials* **2009**, *30*, 3934–3945.
34. Kurosaka, K.; Chen, Q.; Yarovinsky, F.; Oppenheim, J. J.; Yang, D. Mouse Cathelin-Related Antimicrobial Peptide Chemoattracts Leukocytes Using Formyl Peptide Receptor-like 1/Mouse Formyl Peptide Receptor-like 2 as the Receptor and Acts as an Immune Adjuvant. *J. Immunol.* **2005**, *174*, 6257–6265.